

DETERMINATION OF CONCENTRATION BY MEANS OF LIGHT SCATTERING AND DIGITAL IMAGE POSTPROCESSING

Güneş Nakiboğlu¹, Catherine Górlé, Istvan A. Horváth and Jeroen van Beeck

von Karman Institute for Fluid Dynamics, Rhode-Saint-Genese, Belgium

Abstract: The main purpose of this research is to manage simultaneous measurement of velocity and concentration in large cross sections by recording and processing images of cloud structures. Stack gas dispersion in an atmospheric boundary layer (ABL), was chosen as the test case and investigated both experimentally and numerically. Large scale particle image velocimetry (LS-PIV), which records cloud structures instead of individual particles, was used to obtain the velocity field. Light scattering technique (LST) was employed to determine the concentration of the pollutant from the same set of images. In addition, aspiration probe concentration measurements were performed. The test case was also simulated using the CFD solver FLUENT. Comparison revealed that there is a good agreement between the aspiration probe measurements and the CFD results. For the LST measurements, a non-linear relation between concentration and light intensity was observed.

Key words: Concentration measurement, light scattering technique, aspiration probe, ABL, large scale PIV, CFD, Schmidt number.

1. INTRODUCTION

Research on air pollution has reached major interest in the last few decades, resulting in a growing demand for precise modelling of pollutant concentrations, both experimentally and numerically. Although studying the dispersion of gases in complex urban environments is essential and directly related to the life quality and safety of people living and working in such areas, it is more convenient to use a simple geometry for accuracy assessment purposes (Riddle et al., 2004). In the present research project, gas dispersion from a single stack in an atmospheric boundary layer (ABL) is studied, which is a well understood common test case (Beychok, 1994, Raza et al., 2001, Blocken et al., 2008).

The purpose of this research is to investigate simultaneous measurement of velocity and concentration in large cross sections. Such a technique could not only provide a valuable insight into dispersion processes, but would also be a useful tool for the construction of validation data sets for numerical simulations. The goal of this paper is to present the experimental data obtained for the stack gas dispersion phenomenon and to make a comparison with CFD simulations. The measurements were performed in an ABL wind tunnel. The velocity field has been measured with Large Scale-Particle Image Velocimetry (LS-PIV). The concentration field has been obtained from the set of images obtained for the PIV measurements using Light Scattering Technique (LST). In addition aspiration probe concentration measurements were performed. The numerical part of the research was performed using FLUENT 6.3. Special attention was given to proper modelling of ABL using the method proposed by Blocken et al. (2007).

2. WIND TUNNEL AND ATMOSPHERIC BOUNDARY LAYER

The experiments have been conducted in the Wind Gallery, which is an atmospheric boundary layer wind tunnel at the von Karman Institute. This facility is a suction type, low-speed, open-circuit wind tunnel that incorporates an air inlet fitted with honeycombs, meshes and a three-dimensional contraction. The test section is 1 m high, 1.3 m wide and 7 m long. A battery of four ejectors mounted at the back end drives the airflow which can be varied from 0.25m/s to 1.2m/s. Four Irwin vortex generators (Irwin, 1981) were placed at the entrance of the development section. In addition to the spires, a combination of small cubic roughness elements is placed on the floor to control the properties of the induced boundary layer. At the end of the development section, the lower part of the ABL is successfully simulated.

The ABL profiles were measured with a hotwire and for data acquisition a KUSB-3102 module of Keithley Instruments, Inc. was used together with TestPointTM software. The profiles were obtained by measuring approximately 60 points which were highly clustered near the wall region. A sampling rate of 20Hz was used and for each point data was taken during one minute to obtain a correct average. Mean wind and turbulence intensity profiles were measured 10cm upstream of the location of the stack on the symmetry plane of the test section as presented in Figure 1. These profiles were used as boundary conditions for the numerical modeling. The respective parameters of the ABL are presented in Table 1.

Table 1. Main ABL parameters

Free stream velocity (U_∞) [ms^{-1}]	Roughness Reynolds number (Re_*) [-]	Skin friction coefficient (C_f) [-]	Shear velocity (u_τ) [ms^{-1}]	Power-law coefficient (α) [-]	Boundary layer thickness (δ) [mm]
1.1	5.47	0.006	0.057	0.207	510

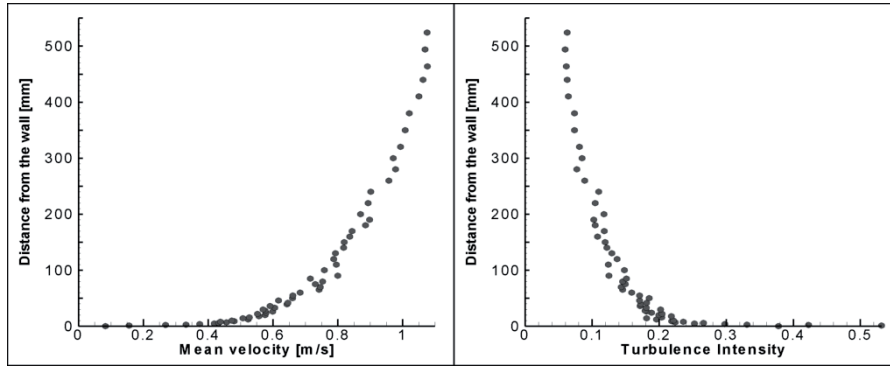


Figure 1. Mean velocity and turbulence intensity profiles.

3. MEASUREMENT TECHNIQUES

Velocity Measurements: Large Scale PIV (LS-PIV)

To determine the velocity field downstream of the stack, LS-PIV has been used such that cloud structures instead of individual particles were imaged. The experimental set-up is presented in Figure 2 (a), the flow was illuminated with a double cavity pulsed Mini:YAG laser. Throughout the experimental campaign, depending on the case, either one or two oil smoke generators were used. One of the smoke generators was employed to seed the upstream flow and the other was used to create a plume from the stack. One spherical and one cylindrical lens with proper focal lengths were used to achieve a well focalized light sheet. During the experiments a PCO Sencicam-12 bit gray scale camera (PCO Imaging) was used with a resolution of 1280×832. The synchronization was managed using the MotionProX timing hub signal generator (IDT Inc).

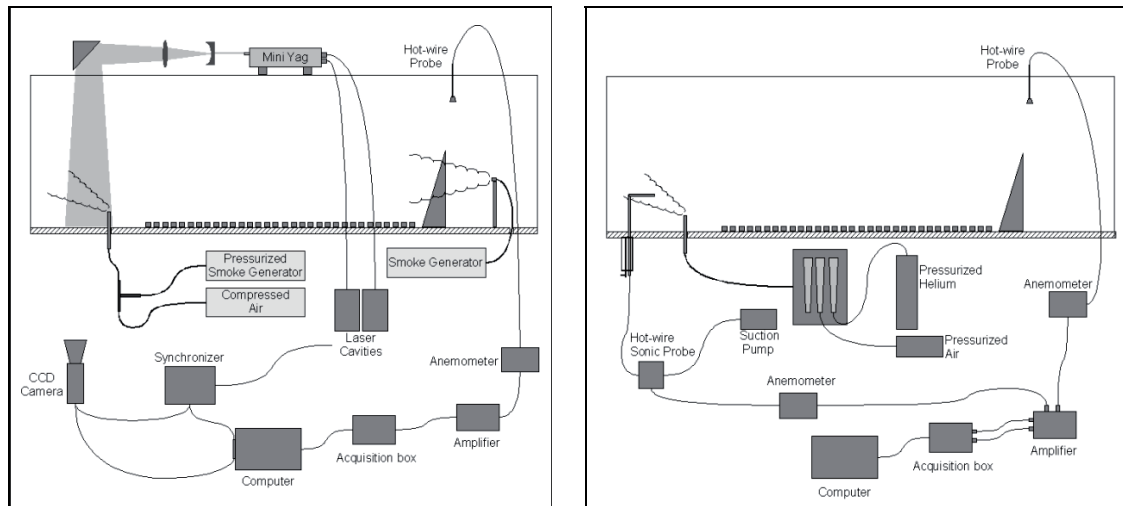


Figure 2. Experimental set-ups for PIV (a) and aspiration probe (b) measurements.

The field of view is approximately $0.3\text{m} \times 0.4\text{m}$ which is quite large compared to standard PIV applications. For the digital image processing of the PIV images, the WIDIM (window displacement iterative multigrid) algorithm developed by Scarano (1997) was used. The average and RMS flow fields were obtained using 500 couples per case. To improve the average quantities, a technique called “*signal to noise ratio filtered averaging*”, was used (Nakiboglu, 2008). In this approach, only validated vectors from each instantaneous field were used in the averaging. The threshold for the signal to noise ratio for a validated vector was chosen as 1.5, which is the default value of WIDIM.

Concentration Measurements: Aspiration Probes Measurements & Light Scattering Technique (LST)

The concentration measurements were performed using two different approaches: aspiration probes and LST.

The aspiration probe is a hot wire, sonic nozzle probe (Maroteaux et al., 1990), which is a reliable, intrusive, point measurement technique. The working principle of this concentration measurement technique is based on the properties of a well-known constant temperature hot-wire sensor combined with a sonic nozzle. By means of a sonic hole the velocity on the wire is fixed so that the hotwire voltage becomes sensitive to composition changes of the fluid. Due to its high traceability in air, Helium was used as the tracer gas. With the help of a calibration box, as shown in Figure 2 (b), the gas mixture coming out of the stack has a known ratio of Helium and air. Throughout the

experiments a mixture of air (90%) and Helium (10% by mass) is introduced from the stack, which shows approximately neutrally buoyant plume characteristics. The exit velocity of the plume is around 4.1m/s. Helium gas measurements are performed at 38 locations. For each point, measurements are taken during one minute with a sampling frequency of 50Hz.

More complete data sets for pollutant dispersion in urban areas could be obtained by measuring concentrations in a plane. 2D laser optical concentration measurements are very favorable in this sense. In general, the intensity of the light scattered from the particles is proportional to the local particle density in the light sheet (van de Hulst, 1957). When introducing seeded air into the unseeded air in the wind tunnel, the number of scattering particles in each unit volume of the flow field will be reduced as the control volume moves downstream of the seeding source and the intensity of the scattered light will diminish proportionally. The same set of images that was acquired and used for the PIV study was used.

The relative concentration was calculated through the following formulation as a function of relative light intensity.

$$\frac{C}{C_s} = \frac{I - I_b}{(I - I_b)_s} \frac{(I_0)_s}{I_0} \quad (1)$$

Where C , C_s and I , I_s are the concentration and light intensity at any point and at the exit of the stack respectively. I_b , $(I_b)_s$ is the background light intensity. I_0 , $(I_0)_s$ is the light intensity of a uniformly seeded background. Using this relation the effect of background light and non-uniformity of the illumination was successfully eliminated. The processing was performed on averaging windows of 10×10 pix size.

4. NUMERICAL SIMULATIONS

Accurate simulation of the ABL has utmost importance to correctly predict the dispersion phenomenon. Thus, initial attention in the numerical simulation was given to the proper modelling of the ABL. The problematic part in the CFD modelling is the correct representation of the effect of the surface roughness elements in the wind tunnel by means of wall functions applied to the bottom of the simulation domain. The resulting vertical profiles of mean wind speed and turbulence quantities should have a zero stream wise gradient, which is referred to as a horizontally homogeneous ABL. The difficulty of achieving such a boundary layer has already been highlighted in the literature (Riddle et al., 2004, Franke et al., 2004). Thus, first a set of 2D simulations was performed to achieve a horizontally homogeneous ABL using the method proposed by Blocken et al. (2007) and Franke et al. (2004).

In this study, the SIMPLE algorithm was used with the standard k- turbulence model. All discretization schemes were set to second order. The simulation was terminated when all residuals dropped at least 8 orders of magnitude. The computational domain is approximately 6 times larger than the experimental domain, to minimize the possible adverse effect of boundary conditions. The height of the first cell was determined as 0.008m considering the required resolution of the ABL. The roughness height was defined as half this value (Fluent User's Guide, 2005). To obtain a horizontally homogeneous ABL, the wall roughness coefficient (Cks) was set to 3.53 by defining a user defined function (UDF) (Blocken et al., 2007). The resulting velocity and turbulent properties at the inlet and the outlet of the computational domain are presented in Figure 3.

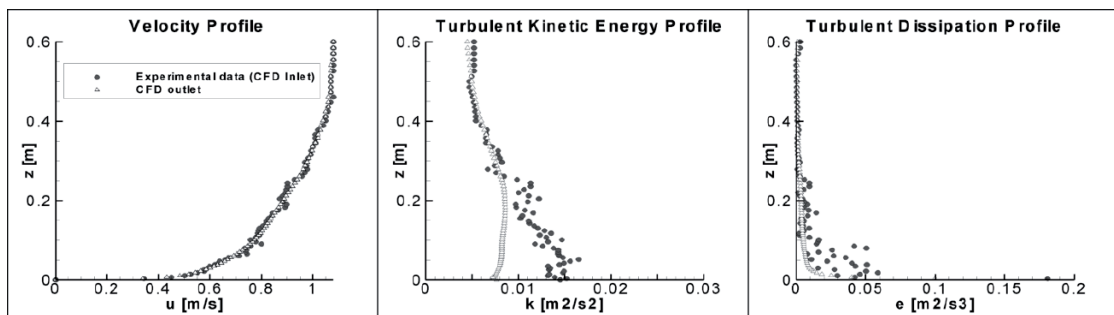


Figure 3. Comparison of velocity and turbulence properties between the inlet and exit planes.

It can be noticed that horizontal homogeneity is achieved for the velocity profile but not for the turbulence properties. In the 3D simulations of the stack gas dispersion, the species transport equations were used, which do not explicitly include the turbulence kinetic energy. Consequently the non-homogeneity of the turbulence kinetic energy will only have a secondary, limited effect on the results.

The 3D model used for the simulations has a length of 0.7 m, width of 0.65 m and height of 0.6 m. The stack is located 0.1m after the inlet and has a height of 0.1m. The model has a symmetry plane through the centreline of the stack in the stream wise direction to decrease the computational load. The grid was constructed by meshing the

ground surface with unstructured quad elements, which were clustered close to the stack. Using the cooper scheme this face mesh was extruded along the height of the domain to obtain 3D elements. The first cell height was identical to the one used for the 2D ABL simulations. Approximately 350000 elements were created with a skewness angle less than 0.4 for all elements. To determine the concentration distribution, species transport calculations were performed by solving Fick's law of diffusion. In turbulent flows the dominant term for diffusion is the turbulent diffusivity coefficient (D_t). This term is determined through μ_t/Sc_b , where the turbulent Schmidt number, Sc_b , has to be defined. The optimum values for Sc_b are widely distributed in a range of 0.2-1.3 and the specific value selected has a significant effect on the results (Tominaga & Stathopoulos, 2007).

5. COMPARISON OF RESULTS

All the vertical profiles presented were taken from the symmetry plane of the stack in the stream wise direction. The region up to 30 stack diameters (D) downstream was investigated in the study, but the results presented here cover only the region close to the stack, up to 10D. In general the remaining part shows similar trends and, where necessary, the differences will be highlighted. From Figure 4 and Figure 5, it is seen that there is a good agreement not only in the mean but also in the fluctuating component of the velocity field. The differences between the extremities of the profiles are higher (15%) in the region close to the stack. This difference can mainly be attributed to the difficulty in the precise determination of the exit velocity from the stack, which is used as a boundary condition in the CFD simulations. The introduction of a large amount of tracer particles, as required to obtain sufficient light scattering for the LST measurements, affects the characteristics of the fluid in which they are suspended and thereby complicates the velocity measurement at the stack exit.

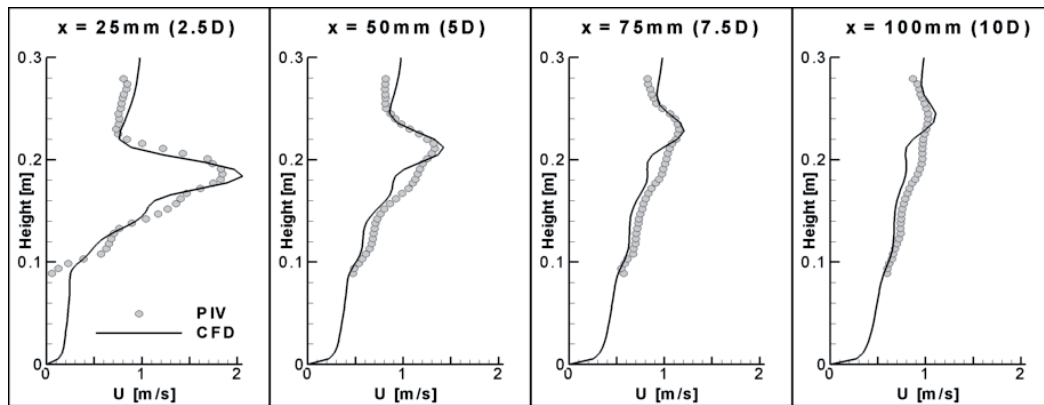


Figure 4. Comparison of velocity magnitudes obtained by PIV and CFD at different downstream locations.

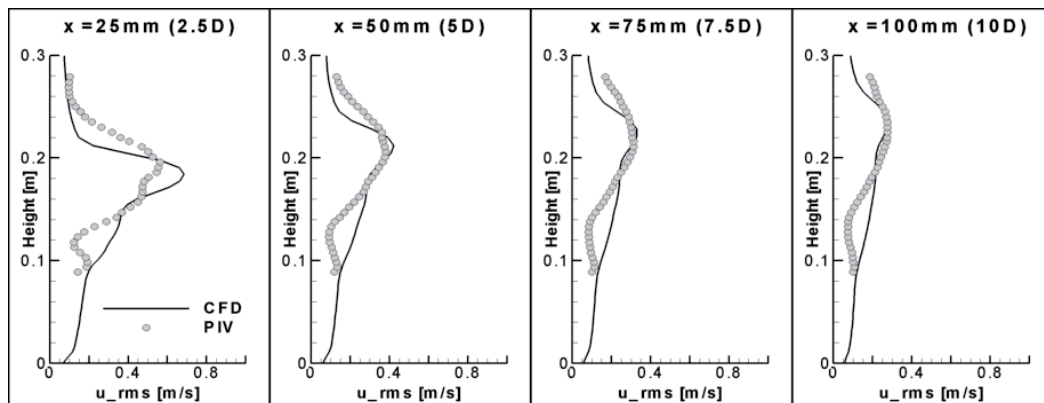


Figure 5. Comparison of fluctuating component of velocity obtained by PIV and CFD at different downstream locations.

A comparison of the aspiration probe measurements and the CFD results is presented in Figure 6. It is noticed that a turbulent Schmidt number of 0.4 gives the best fit as proposed by Di Sabatino et al. (2007). The experimental and numerical data are in agreement within a band of 0.004 by weight ratio. Even smaller values for the turbulent Schmidt number are proposed in literature (Riddle et al., 2004, Tominaga & Stathopoulos, 2007) and could possibly result in a further improvement of the agreement with the test data.

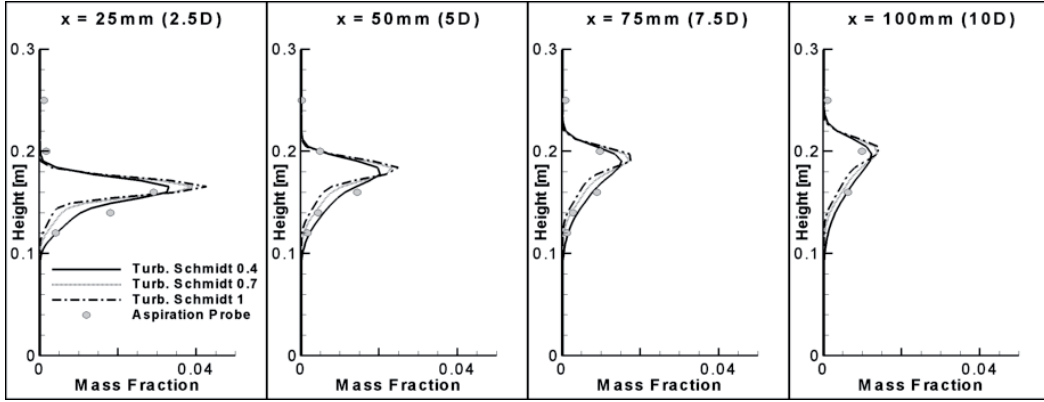


Figure 6. Comparison of concentration obtained by aspiration probe measurements and 3 CFD simulations with different Sc_t .

When comparing the LST measurements with the CFD results as presented in Figure 7, it is noticed that the concentration is over estimated by LST. This is due to the failure of independent scattering, which dictates that the total light observed by the camera is the summation of the scattered light caused by each particle (Borrego, 1978). The phenomenon behind this failure is the absorption and reflection of the scattered light by other particles in the medium. This problem arises when there is an excessive amount of particles in the flow. Thus, the light intensity at the exit of the stack results in an underestimation of the concentration here. Eventually, since the reference concentration is taken at the stack exit, the relative concentration of the flow is overestimated.

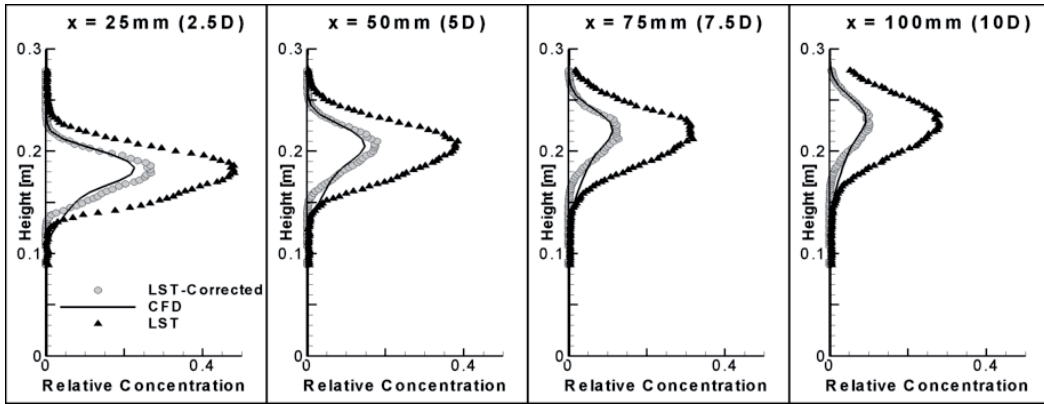


Figure 7. Comparison of concentration obtained by CFD and LST together with a correction proposed for LST measurements.

The concentrations measured by LST and estimated using CFD can be related through a power-law function,

$$\frac{C_{Real}}{C_{Real_0}} = \left(\frac{C_{LST}}{C_{LST_0}} \right)^\alpha \quad (2)$$

Seeking a possible best fit with CFD, the exponent α was determined as 1.8. The improvement in the results with this non-linear correction is seen in Figure 7. However, the proposed correction is only suitable for high concentration regions, because the power-law function has infinite slope near 0, which leads to an over correction at low concentrations. A better correction function should have an exponential nature.

6. CONCLUSION

Through this research, the accuracy of aspiration probes was proved once again. With the proper selection of the turbulent Schmidt number, CFD was able to make an accurate estimation of the concentration field. LS-PIV was employed successfully to determine the average and fluctuating component of the velocity field. It was shown that the same set of images used in LS-PIV can also be used for concentration measurements through LST. Although the accuracy of LST measurements is not as high as aspiration probe measurements, the estimations are still reasonable and can be improved by applying non-linear corrections, as proposed in this study.

REFERENCE

- Beychok, M. R., 1994: Fundamentals of stack gas dispersion. 3rd Edition, Irvine, California.
- Blocken, B., Stathopoulos, T., & Carmeliet, J., 2007: CFD simulation of the atmospheric boundary layer-wall function problems. *Atmospheric Environment*, **41**,238-252.
- Blocken, B., Stathopoulos, T., Saathoff, P., and Wang, X., 2008: Numerical evaluation of pollutant dispersion in the built environment: Comparison between models and experiments. *Journal of Wind Engineering and Industrial Aerodynamics*, (in press).
- Borrego, C., 1978: Local measurements of velocity and concentration. Rhode-Saint-Genese, von Karman Institute for Fluid Dynamics.
- Di Sabatino, S., Buccolieri, R., Pulvirenti, B., and Britter, R., 2007: Simulations of pollutant dispersion within idealised urban-type geometries with CFD and integral models. *Atmospheric Environment*, **41**, 8316-8329.
- Fluent User's Guide, 2005: Fluent Inc.
- Franke, J., Hirsch, C., Jensen, A., Krus, H., Schatzmann, M., Westbury, P., et al., 2004: Recommendations on the use of CFD in wind Engineering. In COST Action C14, Impact of Wind and Storm on City Life Built Environment. *International conference on Urban Wind Engineering and Building Aerodynamics*. Rhode-Saint-Genese, von Karman Institute.
- Irwin, H. A., (1981: The design of spires for wind simulation. *Jour. of Wind Eng. and Industrial Aerodyn.*, 361-366.
- Maroteaux, D., Maroteaux, F., & Murat, M., 1990: Experimental study of a hot wire, sonic nozzle probe for concentration measurements. *Rev. Sci. Instrum.*, **62**, 1057-1062.
- Nakiboglu, G., 2008: Velocity and concentration measurements of a stack gas dispersion in an atmospheric boundary layer. *Project Report*, Rhode-Saint-Genese, von Karman Institute for Fluid Dynamics.
- Raza, S. S., R. Avila and J. Cervantes, 2001: A 3D Lagrangian stochastic model for the meso-scale atmospheric dispersion applications. *Nuclear Engineering Design*, **208**, 15-28.
- Riddle, A., Carruthers, D., Sharpe, A., McHugh, C. and Stocker, J., 2004: Comparison between FLUENT and ADMS for atmospheric dispersion modelling. *Atmospheric Environment*, **38**, 1029-1038.
- Scarano, F., 1997: Improvements in PIV image processing application to a backward-facing step. *Project Report* Rhode-Saint-Genese, von Karman Institute for Fluid Dynamics.
- Tominaga, Y. and T. Stathopoulos, 2007: Turbulent Schmidt numbers for CFD analysis with various types of flowfield. *Atmospheric Environment*, **41**, 8091-8099.
- van de Hulst, H. C., 1957: Light scattering by small particles. New York, John Wiley & Sons.